[Article ID] 1003- 6326(2001)02- 0270- 05

Dry sliding wear of MA/PM Al-10Ti alloy①

WU Jin-ming(吴进明), ZHENG Shi-lie(郑史烈), ZENG Yue-wu(曾跃武), LI Zhi-zhang(李志章)
(Department of Materials Science & Engineering, Zhejiang University, Hangzhou 310027, P. R. China)

[Abstract] Dry sliding wear behaviors of the Al-10Ti alloy prepared by mechanical alloying (MA) were investigated and compared with those of the alloy obtained by the rapid solidification (RS) process. The results show that, under low sliding velocity of 0.66 m/s and low applied load, the predominant wear mechanism of Al-10Ti alloy against carbon steel is adhesion. The fine dispersing reinforcement in the alloy promotes the nucleation and propagation of cracks on the subsurface, leading to a higher wear rate of MA Al-10Ti alloy, compared with that of RS Al-10Ti alloy. With increasing normal load, the formation and spallation of transfer layers on the worn surface become the predominant wear mechanism. Therefore, the wear resistance of the alloy obtained by MA surpasses that achieved by RS due to the higher strength at both ambient and elevated temperature. The wear transfer layer of the MA Al-10Ti alloy is determined to be consisted mainly of Fe_2O_3 and metal Fe.

[Key words] Al-Ti alloy; sliding wear; mechanical alloying; rapid solidification(RS)
[CLC number] TG146.2 [Document code] A

1 INTRODUCTION

Owing to the high specific elastic modulus, high specific strength and excellent mechanical properties both at ambient and elevated temperatures, Al-Ti alloys have found their potential application in the area of aerospace, aircraft and more recently engine parts in automobiles where the anti-wear properties are also required. Up till now, Al-Ti alloys with ideal microstructure of fine Al_3Ti particles dispersing within the Al matrix have been prepared successfully with rapid solidification (RS) and mechanical alloying (MA). These alloys possess excellent mechanical properties and oxidative resistance properties surpassing those of general aluminum alloys, such as Al-8Fe-4Ce and 2014-T6[1~7].

As revealed by many research works, wear resistance of metal matrix composites reinforced with particles (MMC) or short fibers is better than that of matrix alloys[8]. Dry sliding wear behaviors of such composites have been investigated but much is to be done, partly because of the complexity induced by the reinforcements. In our preceding papers, dry sliding wear behaviors of RS Al-Ti alloys and effects of the particle size, particle volume fraction and cold work prior to the wear tests, were reported[9~12].

Al-Ti alloys obtained by MA possess even finer crystalline size and substructure. The MA Al-Ti matrix reinforced with reinforcers of size 100~ 500 nm, compared with that of RS Al-Ti alloys reinforced with reinforcers of size 1~ 3 μm, disperse homogeneously within the Al matrix with high bonding strength between the reinforcer and the matrix[1~6]. Therefore, an improved wear resistance of the alloy can be anticipated. In this paper, dry sliding wear behaviors of the MA Al-10Ti alloy were investigated, and compared with that of the alloy obtained by RS process.

2 EXPERIMENTAL

The preparation procedure of MA and RS Al-10Ti alloy can be found in Refs. [9, 12, 13] respectively. In brief, the RS Al-10Ti alloy was obtained by hot extruding the argon gas atomized alloy powder at 400 ℃ and followed by annealing at 600 ℃ for 100 h. The MA Al-10Ti alloy was achieved by double cold pressing and sintering of the powder which was subjected up to 285 h of ball milling. Typical microstructure of the alloy obtained by RS and MA (designated as RS and MA respectively) is shown in Fig. 1. Table 1 lists the particle size and particle volume fraction, as well as the hardness of the two alloys. The process control agent (stearic acid) added to prevent powder agglomeration during ball milling of the Al-10Ti powder mixture has reacted with Al to form Al_2O_3 and Al_4C_3 particles, as evidenced by many researchers[2~6]. Therefore, the particle volume fraction of MA is larger than that of RS.

Specimens with dimension of 8 mm × 9 mm × 10

Table 1 Particle size, particle volume fraction and hardness of test materials

Preparation method	Particle volume fraction/%	Particle size /μm	HV /MPa
RS	14.0	2.4~ 2.8	657
MA	20.0	0.1~ 0.5	1176

① [Received date] 2000- 04- 10; [Accepted date] 2000- 10- 30

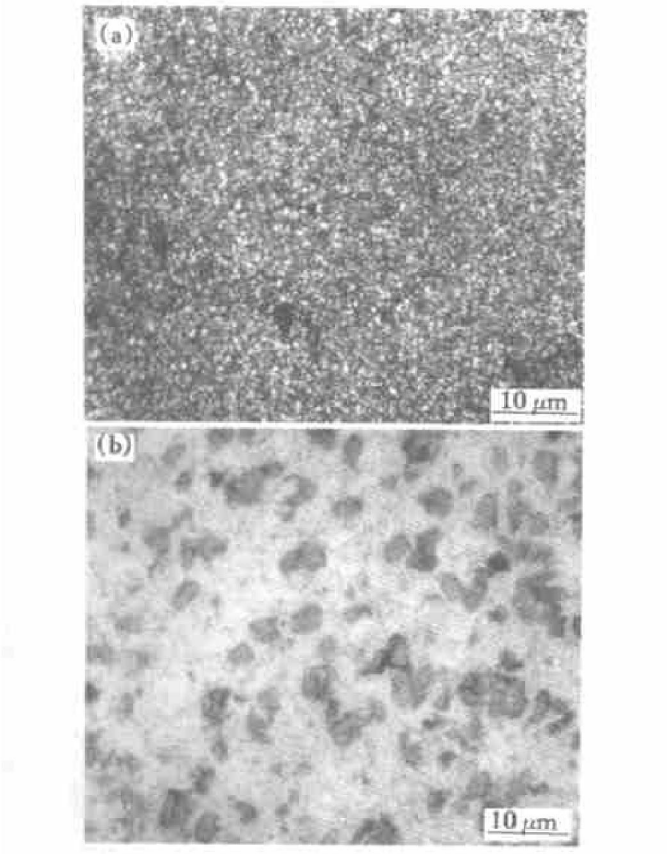

Fig. 1 Typical microstructures of Al-10Ti alloy obtained by MA (a) and RS (b)

mm were subjected to wear tests. The worn surface is 8 mm × 10 mm. Details of the wear tests, conditions of scanning electron microscopy (SEM) and X-ray photoelectron spectra (XPS) analyses were given in Refs. [9, 12]. Here, the sliding velocity was kept constant at a relative low value of about 0.66 m/s.

3 RESULTS

Similar to RS Al-Ti alloys[9, 12], two wear stages, i.e., running-in and steady-state wear stages have been found in the wear volume loss vs sliding distance curves obtained for the MA Al-10Ti alloy. The wear rates of RS and MA calculated by taking the slope of the steady-state wear portion from the curves are found to increase with increasing applied load, as illustrated in Fig. 2. It is also clear that the wear rate of MA is higher than that of RS when the applied load is less than about 12 N, and the reverse is true when the load exceeds 12 N.

Figs. 3, 4 illustrate the worn surfaces of MA at the normal load of 6 N and 15 N, respectively. Similar changes on the worn surface with increased sliding distance can be found under both of the applied load. At the running-in stage, "tongues" like asperities and micro-cracks vertical to the sliding direction can be seen. The size of "tongues" like asperities increased with increasing normal load (comparing Fig. 3(a) to Fig. 4(a)). This suggests that, in the initial wear

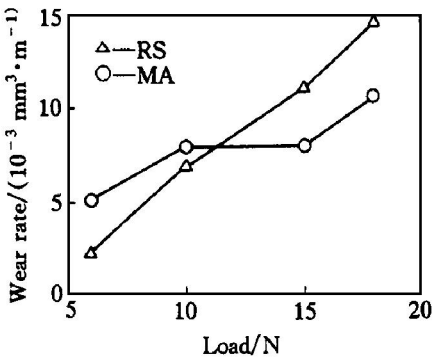

Fig. 2 Relationship between wear rate and applied load

process, lots of shear fracture occurred and the fractured materials between the two counterparts were extruded and curved repeatedly to form plate like debris, as illustrated in Fig. 5(b). In addition, grooves characteristics of abrasive wear were also evidence on the worn surface. When the sliding distance increased, the "tongues" like morphologies disappeared and a much smoother worn surface was obtained (Figs. 3(b), 4(b)). The larger deformation zone, as well as the deeper grooves on the worn surface of the alloy tested at 15 N when compared with that tested at 6 N suggested much severer plastic deformation and abrasive wear with increasing normal load. It should be noted that, despite of the similar morphology of the worn surface, the wear debris generated under the two normal loads were quite different. Dry sliding wear of MA under 15 N of normal load produced mainly fine particles, which is characteristic of the oxidative wear mechanism (Fig. 5(c)). However, a large fraction of plate particles, which is similar to that produced at the running-in wear stage (Fig. 5(b)) consisted the wear debris of MA when tested at 6 N of normal load (Fig. 5(a)). The main wear mechanism of the running-in wear stage of Al-Ti alloys has been determined to be the adhesive wear[9, 12]. This suggests that the wear mechanism of MA worn at low normal load is different from that worn at relatively high normal load. As will be pointed out later, it is the adhesive wear that predominates the sliding wear process when tested at low normal load and low sliding velocity.

Fig. 6 reveals the XPS spectra of the worn surface of RS and MA under the applied load of 15 N. Table 2 lists the composition of the very worn surface with thickness of about 5 nm of MA and RS determined with XPS. The spectra of Fe $2P_{3/2}$ electron for MA are provided in Fig. 7 as an example of the XPS analysis. It is clear that the wear transfer layer of MA, which developed during dry sliding process, was consisted mainly of Fe and Fe_2O_3, while Al_2O_3, minor Fe_2O_3 and TiO_2, made up that of the RS. The iron element dispersed homogeneously on the worn surface of the MA alloy, as revealed by the Fe ele-

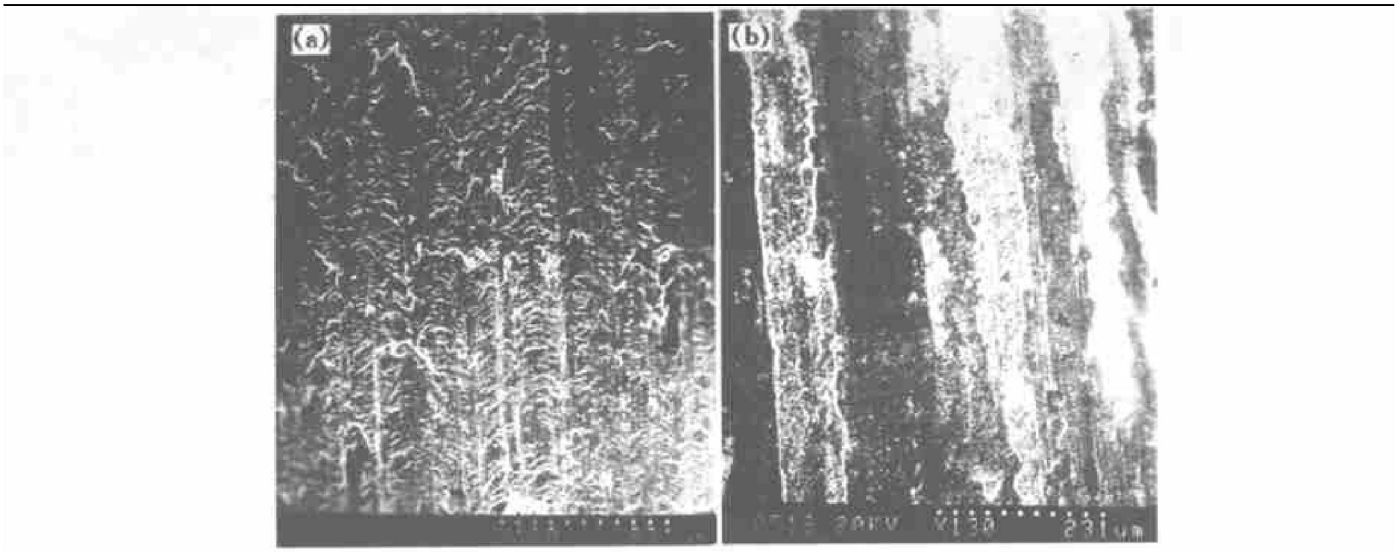

Fig. 3 Worn surfaces of specimen MA under 6 N of applied load
(a) —Running-in stage (sliding distance= 200 m); (b) —Steady-state stage (sliding distance= 3 200 m)

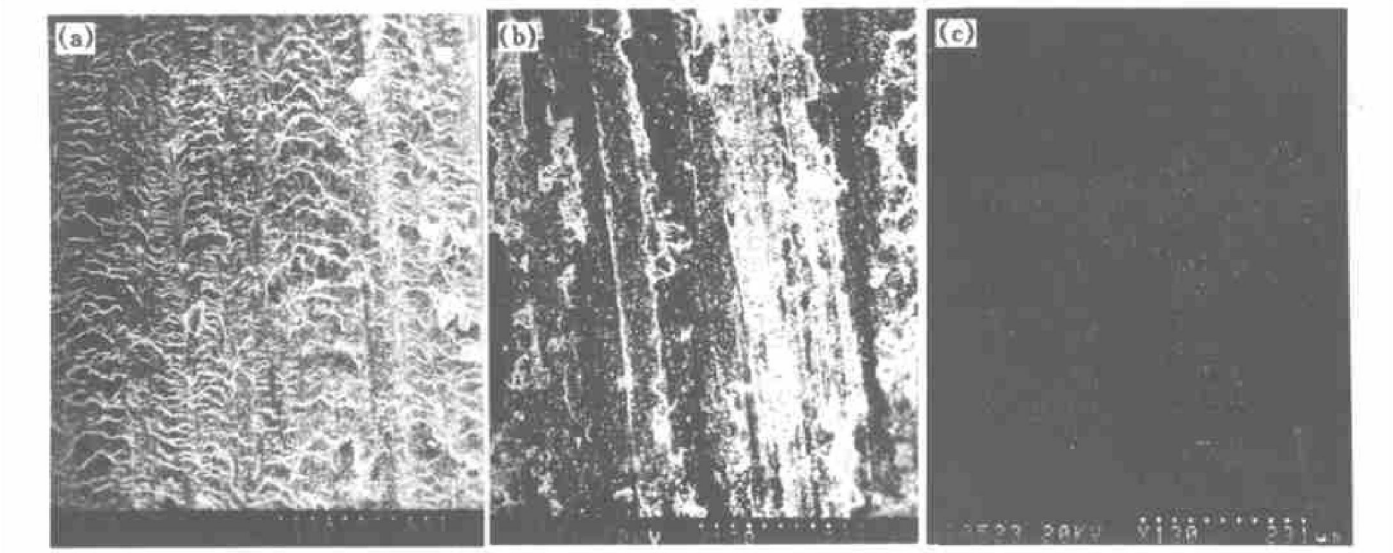

Fig. 4 Worn surfaces of specimen MA under 15 N of applied load
(a) —Running-in stage (sliding distance= 200 m); (b) —Steady-state stage (sliding distance= 3 200 m);
(c) —Fe element dispersion on surface of (b) obtained by EDS

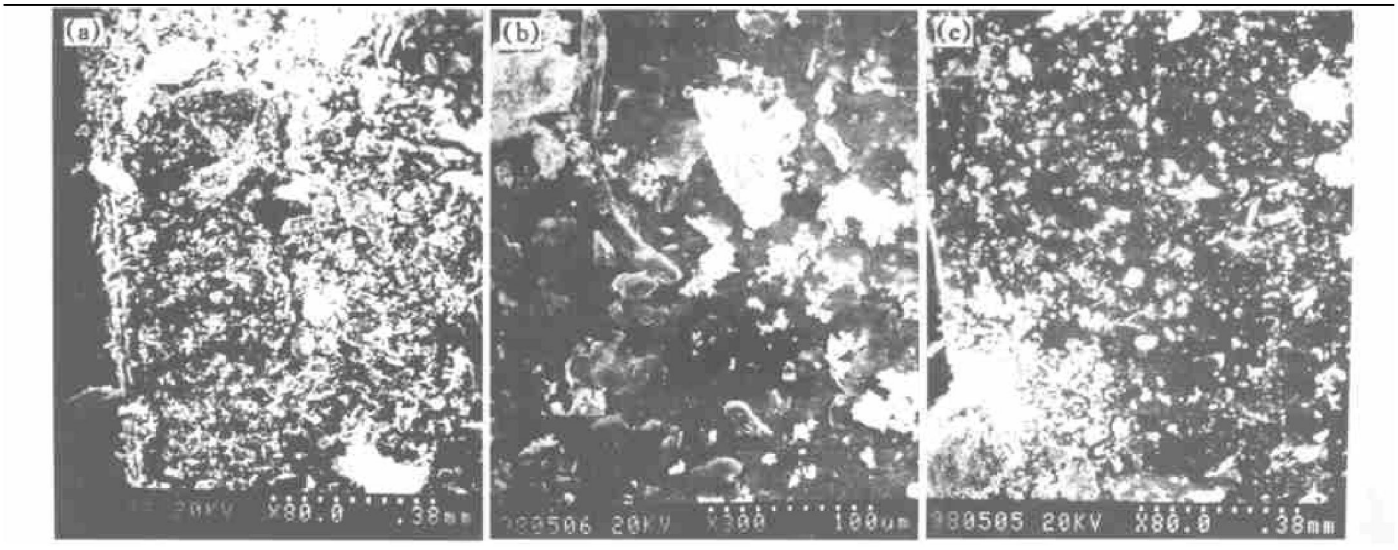

Fig. 5 Wear debris of specimen MA at different normal loads and wear stages
(a) —6 N, steady-state stage; (b) —15 N, running-in stage; (c) —15 N, steady-state stage

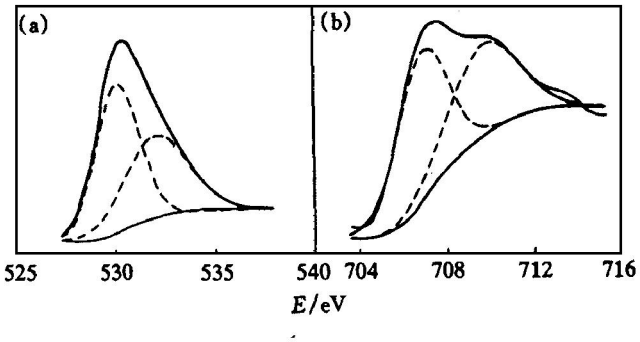

Fig. 6 Spectra of Fe $2P_{3/2}$ (a) and O 1s (b) electron for specimen MA

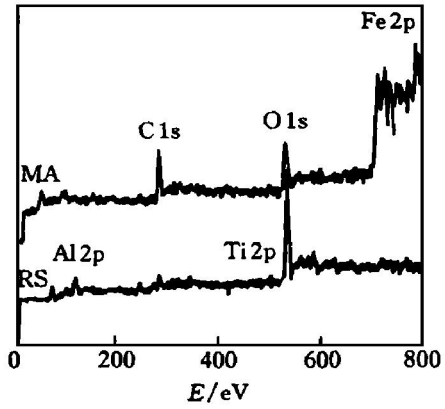

Fig. 7 XPS spectra of worn surface for specimen MA
(load= 15 N; sliding distance= 3 200 m)

ment surface dispersion image, which was obtained by the energy dispersion spectroscopy (EDS) equipped in SEM (Fig. 4(c)). Therefore, it is clear that materials transformation between the specimens and the counterpart steel has occurred. More iron were transferred to the worn surface of MA than RS. Furthermore, it is noted that elemental oxygen existed on the worn surface, which may be the contamination.

4 DISCUSSION

As shown in Table 1, MA possesses finer particle size and higher particle volume fraction, which results in higher hardness. According to the Achard's equation, the dry sliding wear rate Q of materials can be expressed as[14]

$$Q = BW/H$$

where W is the applied load, H is the hardness of materials, B is a constant dependent on local stress, local temperature and chemical reactions on the worn surface etc. However, as can be seen in Fig. 2, although the wear rate of Al-10Ti alloys increases near linearly with increasing applied load, the slope of the fitting line, i.e., B/H does not decrease in accordance to the increase of the hardness. Furthermore, the wear rate of MA is even higher than that of RS when tested at low applied load, despite of its much higher hardness. Therefore, the wear rate of the Al-Ti alloy cannot be attributed to the hardness simply. Effects of the Al_3Ti particle should be highlighted depending on different wear mechanisms.

Table 2 Composition (mole fraction, %) of worn surface of MA and RS
(load= 15 N, sliding distance= 3 200 m)

Specimen	Al	Ti	Fe	O
MA	–	–	33.3	67.7
RS	42.7	0.8	0.4	56.1

At low applied load region (6~ 12 N), temperature rising on the worn surface is not high enough to cause obvious oxidation provided that the sliding velocity of 0.66 m/s in the test is also low. Therefore, adhesion and spallation of materials are the main cause of wear[5,9]. This is supported by the fact that a large fraction of the debris produced is plate-like (Fig. 5 (a)). Although the probability of spot welding between the aluminum alloy and the counter steel is reduced by the improved hardness of MA, it should be noted that, once the welding occurs, materials would spall off readily. The reason is that the fine reinforcements promote the nucleation and propagation of cracks. In addition, higher particle volume fraction and finer particle size result in much higher strain level around the reinforcers[7,11], which in turn decreases wear resistance in the adhesive wear[11,14]. Furthermore, it is clear that abrasive wear also contributes to the loss of materials. Our previous single-point microscopic scratch tests revealed that materials extruded to both sides of the groove by the abrasion do not always spall off the alloy when the alloy possesses good ductility[10]. This means that the softer alloy may not be abraded so readily as generally believed. Meanwhile, the higher volume fraction reinforcer may serve as abrasion, which in turn causes greater mass loss of MA. Therefore, at the low applied load region, the wear rates of MA, which possesses higher hardness, are higher than that of RS. The adhesive wear does not necessarily cause severe wear. In the mild wear stage of the aluminum alloys, the adhesive wear has been reported to be the predominant wear mechanism[15].

Once the applied load exceeds a certain value (12 N in the test), a wear transfer layer, which consists mainly of oxide, will develop on the worn surface. The mass loss of the alloy is affected by the competition between two opposite dynamic processes, i.e., the formation and spallation of the transfer layer[9,12,14]. Al-10Ti alloy prepared by MA possesses higher strength at elevated temperature[2,4], which supports the transfer layer strongly before spalling. Therefore, an increase in the high temperature

strength retards the spalling of the transfer layer, which results in lower wear rates of MA at higher applied load region. The abrasive wear also becomes severe with increasing normal load (Figs. 3, 4) and increasing particle volume fraction. However, the detrimental effect of the reinforcement is surpassed by the beneficial effect as mentioned above.

Different composition of the transfer layers also explains why MA exhibits improved wear resistance at the high normal load region. Under the applied load of 15N, the wear transfer layer of MA is consisted mainly of Fe and Fe_2O_3; while Al_2O_3, minor Fe_2O_3 and TiO_2, make up the transfer layer of the RS. This can be attributed to the higher hardness and higher particle volume fraction of reinforcements for the MA. Once adhesion between two asperities occurs, during sliding of the counter steel, the two welded asperities will fracture on the side of either the counter steel or the alloy. Since the hardness (and thus fracture strength) of MA is higher than that of RS, the possibility for the welded asperities to fracture on the counter steel improves. Meanwhile, the higher volume fraction of particles will serve as abrasion to cut more iron off the counter steel. As a result, for MA, more iron is removed from the counter steel and part of it transfers to the worn surface. Due to the high flash temperature[16], part of the iron transferred to the worn surface reacts with oxygen to form Fe_2O_3. Therefore, it is the iron from the counter steel, rather than Al in the alloy, to be consumed to form the transfer layer during the sliding process. This oxide layer prevents the direct contact of the alloy with the counter steel and serves as in-situ lubrications and thus lowers the wear rate of MA.

5 CONCLUSIONS

1) Under low sliding velocity of 0.66 m/s and low applied load, the predominant wear mechanism of Al-10Ti alloy against carbon steel is adhesion. The fine dispersing reinforcers in the alloy promotes the nucleation and propagation of cracks on the subsurface, resulting in a higher wear rate of MA Al-10Ti alloy, compared with that of RS Al-10Ti alloy.

2) Under low sliding velocity and high applied load, the formation and spallation of transfer layers on the worn surface becomes the predominant wear mechanism. Therefore, the wear resistance of MA Al-10Ti alloy surpass that of RS Al-10Ti alloy due to the higher strength at both ambient and elevated temperature of the alloy.

3) The wear transfer layer of the MA Al-10Ti alloy is mainly consisted of Fe and Fe_2O_3; while Al_2O_3, minor Fe_2O_3 and TiO_2, make up that of the RS Al-10Ti alloy.

[REFERENCES]

[1] Schelleng R D. Mechanical property control of mechanical alloyed aluminum [J]. JOM, 1989, 41: 32.

[2] Wang S H and Kao P W. The strengthening effect of Al_3Ti in high temperature deformation of Al-Al_3Ti composites [J]. Acta Mater, 1998, 46(8): 2675.

[3] Sonawane P W, Krishnaswamy W, Dutta A, et al. Mechanically alloyed Al-10Ti alloy for superplastic forming characteristics [J]. Mater Sci For, 1992, 88-90: 647.

[4] Lee Kwang-Min and Moon Ir-Hyung. High temperature performance of dispersion-strengthened Al-10Ti alloys prepared by mechanical alloying [J]. Mater Sci Eng, 1994, A185: 165.

[5] Lerf R and Morris D G. Mechanical alloying of Al-Ti alloys [J]. Mater Sci Eng, 1990, A128: 119.

[6] Hideki A, Shigeoki S, Tsuyoshi O, et al. Effects of pressure and temperature on consolidation of nanocrystalline MA powder of Al-10.7% ~ 0.6% Fe (mole fraction, %) supersaturated solid solution [J]. Mater Trans JIM, 1997, 38(3): 247.

[7] Wu J M and Li Z Z. Thermal stability and its effects on the mechanical properties of rapidly solidified Al-Ti alloys [J]. Mater Sci Eng, 2000, A289: 246.

[8] Sannino A P and Rack H J. Dry sliding wear of discontinuously reinforced aluminum composite: review and discussion [J]. Wear, 1995, 189: 1.

[9] WU N Q, WANG G X, LI Z Z, et al. Microstructure and sliding wear behavior of PM alloy Al-10Ti after thermal exposure [J]. Wear, 1997, 203-204: 155.

[10] WU Jin-ming, WU Nian-qiang, WANG Guang-xin, et al. In-situ observation of single-point wear of PM Al-Ti alloy [J]. Trans Nonferrous Met Soc China, 1997, 7(3): 69.

[11] WU J M, ZHENG S L, LI Z Z, et al. Effects of cold-deformation on the low speed sliding wear of the RS/PM Al-10% Ti alloy against carbon steel [J]. Wear, 1999, 232(1): 25.

[12] WU Nian-qiang, WU Jin-ming, LIN Suo, et al. Dry sliding wear of PM Al-10Ti alloy [J]. Trans Nonferrous Met Soc China, 1998, 8(3): 421.

[13] WU Jin-ming, WU Nian-qiang, ZENG Yue-wu, et al. Sintering of mechanical alloyed Al-8Ti powder [J]. Heat Treatment of Metals, (in Chinese), 1997, 12: 3.

[14] Lim S C and Ashby M F. Overview No 55: Wear-mechanism maps [J]. Acta Metall, 1987, 35(1): 1.

[15] Sahin Y and Murphy S. The effect of sliding speed and microstructure on the dry wear properties of metal-matrix composites [J]. Wear, 1998, 214: 98.

[16] Razavizadeh K and Eyre T S. Oxidation wear of aluminium [J]. Wear, 1982, 79: 325.

(Edited by HUANG Jin-song)